行政院國家科學委員會補助專題研究計畫成果報告

※※※※※※※※※※※※※※※※※※※※※※※※※
※ ※
※ **階層式 CDMA 行動通信系統之架構設計及性能分析** ※
※ ※
※※※※※※※※※※※※※※※※※※※※※※※※※

計畫類別：■個別型計畫　　□整合型計畫
計畫編號：NSC 91－2213－E－009－068
執行期間： 91 **年** 8 **月** 1 **日 至** 92 **年** 7 **月** 31 **日**

計畫主持人：王蒞君副教授

本成果報告包括以下應繳交之附件：
- □赴國外出差或研習心得報告一份
- □赴大陸地區出差或研習心得報告一份
- ■出席國際學術會議心得報告及發表之論文各一份
- □國際合作研究計畫國外研究報告書一份

執行單位：交通大學電信工程系

中 華 民 國 92 **年** 5 **月** 20 **日**

行政院國家科學委員會專題研究計畫成果報告
階層式 CDMA 行動通信系統之架構設計及性能分析(一)[1]

Spectrum Sharing for Frequency Hopped CDMA Systems with Overlaying Cellular Structures

計畫編號：NSC 90-2213-E-009-068
執行期限：91 年 8 月 1 日至 92 年 7 月 31 日
主持人：王蒞君副教授 交通大學電信工程系
計劃參與人員:陳瓊璋、謝昆瑾、黃晞晏等 交通大學電信工程系

中文摘要

在本篇報告中分析了在跳頻式(frequency hopped)**分碼多工展頻**(CDMA, Code Division Multiple Acces)**階層蜂巢式系統**(HCS, Hierarchical Cellular System)**上鏈路的系統容量：其大細胞和小細胞共用同一個上鏈路頻帶。為了能讓在跳頻式分碼多工展頻階層蜂巢式系統中的大小細胞能順利共用上鏈路頻帶，於是我們研究如何利用跳頻及能量控制**(Power Control)**來減少大小細胞彼此之間的干擾。**

我們在本篇報告中觀察隨機跳頻(Random Frequency Hopping, RFH) **及動態跳頻** (Dynamic Frequency Hopping, DFH) **結合三種能量管理方式後的表現：**(1) **以信號強度為主的能量控制** (2) **不同最大傳送功率的靜態能量設定**(Static Power Setting, SPS) (3) **不做能量控制。經由分析和模擬，可以看到在使用靜能能量設定或能量控制的前題之下，隨機跳頻和動能跳頻的系統都能比頻帶分割的系統服務更多的使用者。**

然而，只有動態跳頻系統可以在不做能量控制的情況下仍然會比頻帶分割系統的情形服務更多的使用者。在某些情況下，隨機跳頻系統會比頻帶分割系統在服務人數上的表現來的差。

關鍵詞： 階層式架構, 隨機跳頻, 動態跳頻, 頻帶分割, 能量控制。

Abstract

This paper analyzes the uplink capacity of a frequency hopped CDMA system with spectrum sharing between a hot spot microcell embedded in an overlaying macrocell. We investigate how frequency hopping can function together with power control in order to allow the same frequency spectrum to be shared between the two tiers in the CDMA hierarchical cellular system. We consider random frequency hopping (RFH) and dynamic frequency hopping (DFH) combined with three power management methods: 1) signal strength based dynamic power control (PC), 2) static power setting with different maximum transmit power constraints (SPS), and 3) no power control (NPC). Through analysis and simulation, we demonstrate that when employing either the SPS or the PC methods, frequency sharing with DFH outperforms frequency sharing with RFH in terms of system capacity. Both frequency sharing schemes provide larger capacity than splitting frequency band between macrocells and microcells. However, without using any power management methods, only frequency sharing with DFH can still perform better than the frequency splitting approach. In some cases frequency sharing with RFH may even have lower capacity than frequency splitting.

Keywords : Hierarchical cellular system (HCS), random frequency hopping (RFH), dynamic frequency hopping (DFH), frequency split (FS), and power control (PC).

---

[1] **本文已在** IEEE VTC Spring 2003 **刊登，詳細內容如附件。**

行政院國家科學委員會專題研究計畫成果報告
階層式 CDMA 行動通信系統之架構設計及性能分析(二)[1]

Interference Analysis of TDD-CDMA Systems with Directional Antennas

計畫編號：NSC 90-2213-E-009-068
執行期限：91 年 8 月 1 日至 92 年 7 月 31 日
主持人：王蒞君副教授 交通大學電信工程系
計劃參與人員:陳瓊璋、謝昆瑾、黃晞晏等 交通大學電信工程系

中文摘要

在本篇報告中我們探索在提供非對稱網路服務的劃碼多重進接(CDMA, Code Division Multiple Access)**展頻系統中使用指向性天線的優點，由於在分時多工模式中來自其他細胞的干擾**(Intercell Interference)**會減低系統的容量，在使用全向性天線的系統中，人們提出許多分配上、下鏈路時槽**(Time Slot)**的演算法來減少基地台接收來自其他基地台的干擾。然而這些方法多半需要控制所有基地台中每一個上、下鏈路時槽的分配，明顯地，這限制住原本分時多工系統所能提供不同上下行頻寬的能力。**

在本研究報告中，我們將原本一個細胞使用一全向性天線的系統用一個細胞中有三個指向性天線的系統取代。在分析這種系統下彼此干擾的情況後，可以發現指向性天線在空間上帶來更多的自由度去分配上、下鏈路時槽，因此這方法讓分時多工的系統更能提供各種不同上、下鏈路頻寬要求的服務。

關鍵詞：分時雙工，非對稱服務，干擾分析

Abstract

This paper explore the advantages of using directional antennas for TDD-CDMA systems to support the asymmetric traffic. Because the intercell interference may degrade system capacity, many slot allocation algorithms are proposed to avoid cross slot interference for omni-directional cellular system. These algorithms typically require a global control on the transmission direction in each time slot. Apparently, this requirement substantially limits the capability of TDD system to enable different rate asymmetry in different cells.

Instead of considering omni-directional antennas, this paper proposes to use the tri-sector cellular architecture with three directional antennas employed at each base station. We analyze the interference of this kind of TDD-CDMA system using directional antennas and find that the directivity of directional antenna provides an additional degree of freedom in allocating slot resource. This advantage enables the TDD-CDMA system to support asymmetry uplink and downlink traffics with different rate of asymmetry among neighboring cells.

Keywords : Time Division Duplex (TDD), CDMA system, Asymmetric Services, Interference Analysis.

[1] **本文已在投稿** IEEE VTC Fall 2003**，詳細內容如附件。**

行政院國家科學委員會專題研究計畫成果報告
階層式 CDMA 行動通信系統之架構設計及性能分析(三)[1]

An Analytical Framework for Capacity and Fairness Evaluation in High Speed Wireless Data Networks

計畫編號：NSC 90-2213-E-009-068
執行期限：91 年 8 月 1 日至 92 年 7 月 31 日
主持人：王蒞君副教授 交通大學電信工程系
計劃參與人員:陳瓊璋、謝昆瑾、黃晞晏等 交通大學電信工程系

中文摘要

在本篇報告中我們提出一個高速無線數據網路的系的性能驗證平台，在這平台中，系統的容量以及用戶的公平性的議題都可以被分析與估算。

在實體層方面，我們的模型同時考慮到了電波傳播路徑耗損(propagation path loss)**、慢速時變的遮蔽效應**(shadowing)**、以及快速時變的通道衰落效應**(fading)**。在網路層方面，我們的平台可以允許使用不同的排程**(scheduling)**演算法，並可以模擬不同用戶之間的因不同資料需求量對系統效能所產生的影響。**

簡言之，在我們所提出的平台中，我們可以分析在真實無線通道環境、非均勻用戶資料需求量、以及不同的排程演算法下的系統容量以及用戶公平性。從結果中可得知，在一個使用排程技術的無線通信數據網路中，不僅無線通道環境的變化對系統性能有重要影響，非均勻用戶資料需求量的分布也會對結果有所影響。

關鍵詞： 排程演算法，容量與公平性，非均勻用戶資料需求量

Abstract

This paper presents an analytical framework to evaluate the downlink capacity and fairness performance for high speed wireless data networks from both the physical layer and the network layer perspectives. From the physical layer standpoint, we take into account of propagation loss, log-normal shadowing and Nakagami fading. From the network layer perspective, we model different scheduling policies and the impact of nonuniform traffic intensity of mobile users into our framework. We analyze the joint effects of radio channel impairments, nonuniform traffic intensity and scheduling algorithms on the downlink capacity and fairness performance of wireless data networks based on the developed framework. Our results suggest that it is crucial for wireless scheduling algorithms to consider not only the radio channel impairments, but also the traffic intensity distribution in the whole network.

Keywords : Scheduling algorithm, capacity and fairness, nonuniform traffic intensity

---

[1] **本文已投稿** IEEE Globecom 2003**，詳細內容如附件。**

Spectrum Sharing for Frequency Hopped CDMA Systems with Overlaying Cellular Structures

Li-Chun Wang and Kuan-Jiin Shieh
Department of Communication Engineering
National Chiao Tung University
1001 Tahsueh Rd., Hsinchu, Taiwan 30050, ROC
Tel: +886-3-5712121 ext. 54511, Fax: +886-3-5710116
lichun@cc.nctu.edu.tw

Abstract – This paper analyzes the uplink capacity of a frequency hopped CDMA system with spectrum sharing between a hot spot microcell embedded in an overlaying macrocell. We investigate how frequency hopping can function together with power control in order to allow the same frequency spectrum to be shared between the two tiers in the CDMA hierarchical cellular system. We consider random frequency hopping (RFH) and dynamic frequency hopping (DFH) combined with three power management methods: 1) signal strength based dynamic power control (PC), 2) static power setting with different maximum transmit power constraints (SPS), and 3) no power control (NPC). Through analysis and simulation, we demonstrate that when employing either the SPS or the PC methods, frequency sharing with DFH outperforms frequency sharing with RFH in terms of system capacity. Both frequency sharing schemes provide larger capacity than splitting frequency band between macrocells and microcells. However, without using any power management methods, only frequency sharing with DFH can still perform better than the frequency splitting approach. In some cases frequency sharing with RFH may even have lower capacity than frequency splitting.

Keywords: Hierarchical cellular system (HCS), random frequency hopping (RFH), dynamic frequency hopping (DFH), frequency split (FS), and power control (PC).

I. INTRODUCTION

How to improve system capacity is always an important issue in wireless networks. Deploying hierarchical cellular system (HCS) is one of the solutions to increase system capacity. In hierarchical cellular systems, macrocells are responsible for extending coverage area, while the microcells are aimed to serve the areas with high user density. To make both macrocells and microcells share the same frequency is a challenging task because the mutual interference exists between macrocells and microcells.

In this paper, we examine how frequency hopping can reduce the interference between the two tiers in hierarchical cellular system, with sharing the same spectrum between macrocells and microcells. In [1], one can see that the design of frequency hopping pattern have severe impacts on system capacity. In this paper, we will compare three frequency utilization schemes: 1) frequency sharing with random frequency hopping (RFH) [1-2], 2) frequency sharing with dynamic frequency hopping (DFH) [1-2], and 3) frequency split (FS). Furthermore, we will evaluate the effect of three different transmission power management methods on system capacity, including 1) no power control (NPC), 2) static power setting with different maximum transmission power constraints (SPS), and 3) power control (PC).

The purpose of this paper is to determine the uplink capacity of a hierarchical CDMA frequency hopped cellular system with three frequency utilization schemes and three transmission power managements by analysis and simulation. In [3], one can see that the system capacity of a HCS with RFH is less than that of a HCS with frequency splitting. In this paper, we will show that if frequency hopping patterns are designed more carefully, sharing all available frequency spectrums between macrocells and microcells can have larger system capacity than splitting the spectrum. We also propose a simple power management method by setting the user terminal's transmission power to the two different fixed values at the macrocell and the microcell. This simple static power setting approach can have the same performance as dynamic power control in frequency hopped CDMA system in terms of capacity.

The rest of this paper is organized as follows. Section II describes propagation model, traffic model, frequency utilization, and transmission power management methods. In Section III, we analyze system capacity. Section IV shows the simulation and analytical results. In Section V, we will give our conclusions.

II. SYSTEM MODEL

In this section, we describe the system model including propagation model, frequency utilization, and transmission power management methods.

*This work was supported jointly by the National Science Council, Taiwan, R.O.C, under the contracts 91-2219-E-009-016 and 90-2213-E-009-068, and MOE Program for Promoting Academic Excellence of Universities under the grant number Ex-91-E-FA06-4-4, and 89-E-FA06-2-4.

A. Propagation Model

We usually characterize wireless cannels by path loss, shadowing, and fading. Path loss is a function of the distance between a base station and a mobile station. The path-loss exponent used in this paper is four [4]. Shadowing is modeled as a normal random variable in the dB domain. The standard deviations of shadowing are set to be 4 dB for a microcell and 8 dB for a macrocell [5].

B. Frequency Utilization

We consider three frequency utilization schemes: 1) frequency sharing with random frequency hopping (RFH), 2) frequency sharing with dynamic frequency hopping (DFH) and 3) frequency splitting with random frequency hopping (FS). We assume that a base station coordinates all frequency hopping patterns within a cell, thereby avoiding intra-cell interference. For the RFH scheme, because its frequency hopping pattern is random, there is no frequency coordination among cells. For the DFH scheme, the base station will choose the frequencies with better SIR quality and use these frequencies in its hopping pattern. When a base station manages its frequency patterns, it will avoid choosing the frequencies that have been used by other cells. For the frequency splitting scheme, because a microcell uses different frequency spectrum from a macrocell, there is no inter-cell interference between the microcell and the macrocell.

C. Transmission Power Managements

We discuss three mobile station transmission power management methods in this paper: 1) no power control (NPC), 2) static power setting (SPS), and 3) power control (PC). For the NPC method, all mobile stations transmit the same power, no matter if a mobile station belongs to a microcell or a macrocell. In this case, we set the transmission power to be the power level that is required at the cell boundary with consideration of a shadowing margin. For the SPS scheme, the static power level of the macrocell user is different from that of the microcell user. Specifically, the transmission power of a microcell user is usually less than that of a macrocell user because the distance from a mobile terminal to a microcell base station is usually shorter than that to a macrocell base station. For the PC scheme, all the mobile terminals in a cell have the same received signal power at the serving base station by adjusting its transmission power to compensate path loss and shadowing.

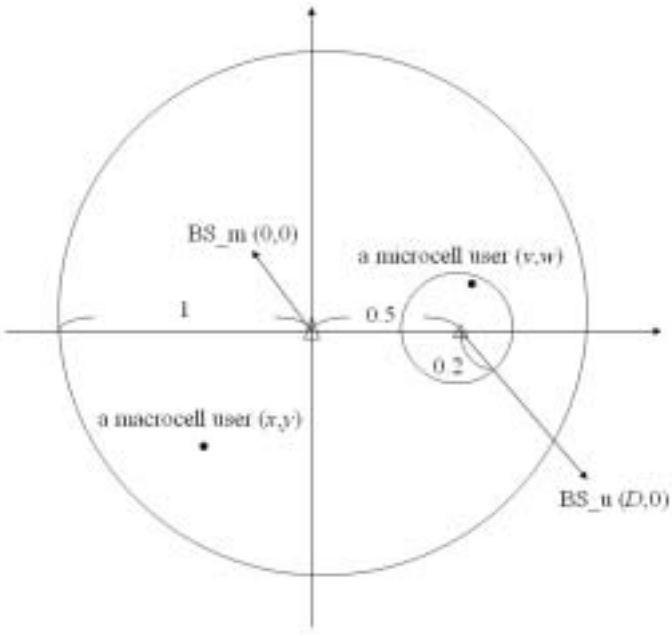

Figure 1: The considered hierarchical cellular system.

III. ANALYSIS

To analyze the performance of frequency hopped CDMA systems, there are two important issues. One is the expected value of frequency collisions, and the other is the signal-to-interference of the collided frequencies.

A. Average Frequency Collisions

1) Random Frequency Hopping (RFH)

For the RFH scheme, there is no intra-cell interference in each cell, but there still exists inter-cell interference. We can find the expected value of frequency collisions for the RFH scheme as follow:

$$E\left[N_{freq.collision}\right]=\sum_{i=\max\{0,\mu+M-T\}}^{i=\min\{\mu,M\}} i*\frac{\binom{T}{\mu}*\binom{\mu}{i}*\binom{T-\mu}{M-i}}{\binom{T}{\mu}*\binom{T}{M}} \quad (1)$$

where μ denotes the number of the microcell mobile stations, and M denotes the number of the macrocell mobile stations. The symbol T denotes the total number of available frequencies.

2) Dynamic Frequency Hopping (DFH)

For the DFH scheme, frequency collisions occur when the sum of microcell users and macrocell users is greater than the total available frequencies. Denote the number of the frequency collisions as $i_{collision}$. Then

$$i_{collision}=\begin{cases}\mu+M-T & , \ when\ \mu+M>T\\ 0 & , \ otherwise\end{cases}, \quad (2)$$

where μ, M, and T are defined in (1).

3) Frequency Split (FS)

In the FS scheme, there is no inter-cell interference because a microcell and a macrocell use different frequencies.

B. Average SIR in dB

Now, we analyze the probability that the received SIR is less than the required SIR threshold (denoted as SIR_T) when a frequency collision occurs. First, we find the expected value of SIR in decibels considering only path loss. Second, we incorporate log-normal distributed shadowing and view SIR as another log-normal distributed random variable. Third, we find the probability of SIR that is less than SIR_T.

1) No Power Control (NPC)

Denote C as the transmission power of a mobile station including path loss and shadowing margin. Then, C can be written as

$$C = \max\left\{\frac{R_\mu{}^4 * S}{H_\mu}, \frac{R_M{}^4 * S}{H_M}\right\} * M_\chi \quad , \tag{3}$$

where R_μ and R_M denote the radii of a microcell and a macrocell, respectively; S denotes the required received power; H_μ and H_M denote the antenna heights of a microcell and a macrocell; and M_χ denotes a shadowing margin. We express the desired signal P_S and interference P_I at a microcell base station as follows:

$$P_S = \frac{C}{\left(x^2 + y^2 + h_\mu{}^2\right)^2} * \chi_4 \tag{4}$$

and

$$P_I = \frac{C}{\left((v-D)^2 + w^2 + h_\mu{}^2\right)^2} * \chi_4 \quad , \tag{5}$$

where C is the transmission power defined in (3), D denotes the distance between a microcell base station and a macrocell base station, (x,y) and (v,w) are the positions of a microcell mobile station and that of a macrocell mobile station, respectively. The microcell base station and the macrocell base station are positioned at $(D,0)$ and $(0,0)$, respectively. The symbol, χ_4, is a shadowing component with standard deviation of 4 dB. Then we can get the expected value of SIR as follow:

$$\overline{SIR(dB)} = \int_{-R_\mu}^{R_\mu} \int_{-\sqrt{R_\mu{}^2 - x^2}}^{\sqrt{R_\mu{}^2 - x^2}} \int_{-R_M}^{R_M} \int_{-\sqrt{R_M{}^2 - v^2}}^{\sqrt{R_M{}^2 - v^2}} \frac{1}{\pi * R_\mu{}^2} * \frac{1}{\pi * R_M{}^2} * 10 * \log_{10}\left[SIR_{\mu.NPC}\right](dxdy)(dvdw) \quad , \tag{6}$$

TABLE I
THE SHADOWING STANDARD DEVIATION OF SIR FOR THE CONSIDERED CASE

	NPC	SPS	PC
Microcell	$4\sqrt{2}$	$4\sqrt{2}$	$4\sqrt{5}$
Macrocell	$8\sqrt{2}$	$8\sqrt{2}$	$4\sqrt{5}$

where $SIR_{\mu.NPC} = \frac{\left((v-D)^2 + w^2 + h_\mu{}^2\right)^2}{\left(x^2 + y^2 + h_\mu{}^2\right)^2}$. (7)

For the NPC scheme, the SIR at a macrocell can be expressed as

$$SIR_{M.NPC} = \frac{\left((x+D)^2 + y^2 + h_M{}^2\right)^2}{\left(v^2 + w^2 + h_M{}^2\right)^2} \quad . \tag{8}$$

By replacing the $SIR_{\mu.NPC}$ in (6), we can get the average SIR with different transmission power management methods.

2) Static Power Setting (SPS)

Denote $SIR_{\mu.SPS}$ and $SIR_{M.SPS}$ as the received SIR in a microcell and that in a macrocell with the static power setting (SPS) scheme, respectively. Recall in Section II that the SPS scheme results in different maximum transmission power levels for microcell users and macrocell users. Then $SIR_{\mu.SPS}$ and $SIR_{M.SPS}$ can be expressed as

$$SIR_{\mu.SPS} = \frac{\left((v-D)^2 + w^2 + h_\mu{}^2\right)^2}{\left(x^2 + y^2 + h_\mu{}^2\right)^2} * \frac{H_M}{H_\mu} * \left(\frac{R_\mu}{R_M}\right)^4 \tag{9}$$

and

$$SIR_{M.SPS} = \frac{\left((x+D)^2 + y^2 + h_M{}^2\right)^2}{\left(v^2 + w^2 + h_M{}^2\right)^2} * \frac{H_\mu}{H_M} * \left(\frac{R_M}{R_\mu}\right)^4 \tag{10}$$

where H_m, H_μ, R_M, and R_μ have been defined in (3).

3) Power Control (PC)

For the PC scheme, all the mobile stations within a cell have the same received power at a base station. Then the SIR at a microcell, $SIR_{\mu.PC}$, and a macrocell, $SIR_{M.PC}$, can be written as

$$SIR_{\mu.PC} = \frac{\left((v-D)^2 + w^2 + h_\mu{}^2\right)^2}{\left(v^2 + w^2 + h_M{}^2\right)^2} * \frac{H_M}{H_\mu} \tag{11}$$

and

$$SIR_{M.PC} = \frac{\left((x+D)^2 + y^2 + h_M{}^2\right)^2}{\left(x^2 + y^2 + h_\mu{}^2\right)^2} * \frac{H_\mu}{H_M} \quad . \tag{12}$$

C. Impact of Shadowing

Let σ_S and σ_I be the standard deviations of the log-normal distributed shadowing component of the desired signal P_S and the interference P_I, respectively. Assume that P_S and P_I are mutually independent. Then the shadowing component P_S /

P_I can be expressed as another log-normal random variable with a standard deviation, $\sigma_{SIR} = \sqrt{\sigma_S^{\,2} + \sigma_I^{\,2}}$. The standard deviations of the SIR with different power control schemes are listed in Table I. With the standard deviation in Table I and the average SIR, we can define a new normal random variable for SIR. Then, the service outage probability, i.e. the probability of SIR less than SIR_T can be written by

$$P[SIR < SIR\_T] = \frac{1}{2}\left[1 + erf\left(\frac{SIR\_T - \overline{SIR(dB)}}{\sigma_{SIR} * \sqrt{2}}\right)\right] \quad (13)$$

where $erf(x) = \frac{2}{\sqrt{\pi}} \int_0^x e^{-t^2} dt$, $\overline{SIR(dB)}$ is the average SIR, and σ_{SIR} is the standard deviation of SIR defined in Table I.

D. System Capacity

With the information of the probability of frequency collision and the probability of SIR less than SIR_T, we can get the probability of transmission failure by multiplying these two probabilities. We define $W_{\{\mu,M\}}$ as follows:

$$W_{\{\mu,M\}} = \begin{cases} 1, & \text{the system can support } \mu \text{ microcell users and } M \text{ macrocell users with acceptable quality;} \\ 0, & \text{otherwise.} \end{cases} \quad (14)$$

Note that $W_{\{\mu,M\}}$ is related to the collision probability, the service outage probability, and the failure rate threshold we will define in Section IV. Then the system capacity can be approximated as follow [5-6]:

Prob{ Supporting N users successfully}

$$= \sum_{\mu=0}^{N} \binom{N}{\mu} P_h^{\,\mu} (1 - P_h)^{N-\mu} W_{\{\mu,M\}} \quad , \quad (15)$$

where N is the total number of mobile stations, μ is the number of microcell users, M is the number of macrocell users, and P_h is the probability that a mobile station is served by a microcell. In this paper, we require Prob{ Supporting N users successfully } to be larger than 0.95.

IV. Numerical Results

Through simulation, we obtain numerical results to justify the correctness of the analytical model. We consider the system parameters of Table II in our simulation. Note that we assume mobile stations are uniformly distributed in each cell [4]. We define P_h as the probability that a mobile station appears in the microcell area. For the RFH and DFH schemes, the microcell and the macrocell share all the 64 frequencies, but for the FS scheme, microcells use 32 frequencies, and macrocells use the other half. We define packet failure as the event when frequency collision occurs and its measured SIR is below SIR_T.

TABLE II
System Parameters

System		Single microcell and single macrocell
Total available frequencies		64
Mobile station distribution		Uniform
The probability that a mobile station appears in the microcell, P_h		0.5
Distance between the microcell and the macrocell		0.5 km
The ratio of macrocell and microcell antenna gain		10
SIR threshold		7 dB
Transmission failure rate threshold		0.2
The radii of cells	microcell	macrocell
	0.2 km	1 km
The antenna heights	7.5 m	58.5 m
The shadowing deviation standard	4 dB	8 dB

TABLE III
Comparison of $\overline{SIR(dB)}$ with Different Power Control Schemes

	microcell		macrocell	
	Ana.	Sim.	Ana.	Sim.
NPC	30.04	30.04	-3.43	-3.43
SPS	12.08	12.07	14.53	14.54
PC	11.98	11.98	14.64	14.63

A. The Expected Value of the Received SIR in dB

Table III lists the expected value of the received SIR according to (6)-(12) with consideration of only path loss. These results will be used later to calculate the SIR when frequency collision occurs. For the case without power control, one can find that the microcell has better SIR than the macrocell. It indicates that the resource allocation is not quite fair between microcells and macrocells based on the NPC scheme.

TABLE IV
SIR OUTAGE PROBABILITY WITH
DIFFERENT POWER CONTROL METHODS

	Microcell		macrocell	
	Ana.	Sim.	Ana.	Sim.
NPC	0.0002	0.0552	0.8216	0.7784
SPS	0.1844	0.3365	0.2527	0.3071
PC	0.2889	0.3346	0.1965	0.2787

B. SIR Outage Probability

Table IV shows the SIR outage probability according to (13). From Table IV, one can still find that the unfairness exists for the case without power control. The information of SIR outage probability in Table IV will be used to calculate the system capacity later.

C. System Capacity

Figure 2 compares system capacity when frequency hopping and power control are adopted. One can find that frequency sharing with DFH performs better than frequency sharing with RFH. This is because the probability of frequency collision is lower for the DFH system compared to the RFH system. Compared to RFH, DFH can improve the capacity by 196%, 35%, and 35% for the NPC, SPS, and PC schemes, respectively. With either SPS or PC, both the RFH and DFH schemes outperform the frequency splitting case. Without any power management, only DFH can have higher capacity then the frequency splitting case, while the frequency sharing with RFH can even has a lower capacity than frequency splitting. Noteworthily, a simple static power setting with different maximum transmission power constraints is as effective as the signal strength based dynamical power control, which can enable the frequency hopped CDMA systems to share the spectrum in an overlay structure. The difference between analysis and semi-analysis is only in the part of SIR outage probability. In the analysis method, the SIR outage probability is gotten from the analysis result of Table IV, but in the semi-analysis method, the SIR outage probability is gotten from the simulation result of the same table.

V. CONCLUSION

We have analyzed the uplink capacity of a frequency hopped CDMA systems in an overlaying cellular structure with spectrum sharing between a hot spot microcell and an overlaying macrocell. We find that if frequency hopping patterns can be designed more carefully, sharing all frequency spectrums between macrocells and microcells can have larger system capacity than splitting the spectrum. We also find that combining power control and frequency hopping is critical to achieve the goal of sharing spectrum between microcells and macrocells in a hierarchical CDMA cellular system.

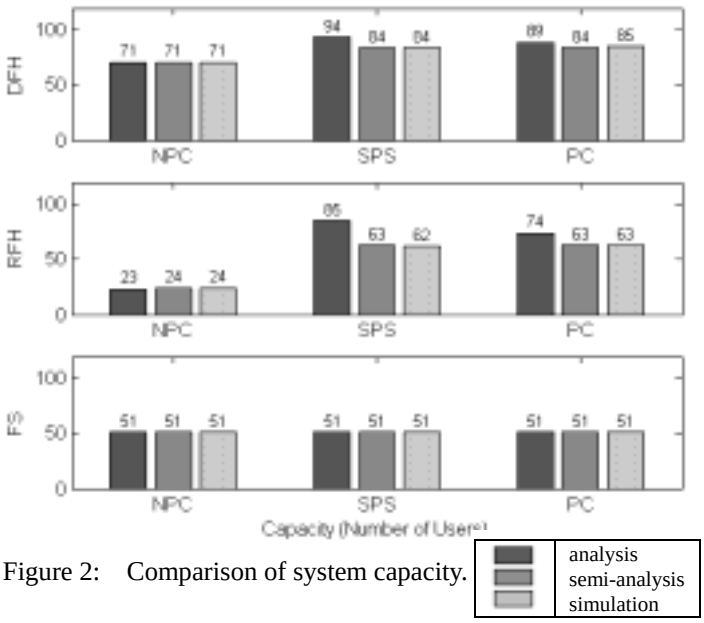

Figure 2: Comparison of system capacity.

REFERENCE

[1] Z. Kostic, I. Maric, and X. Wang, "Fundamentals of dynamic frequency hopping in cellular systems", IEEE Journal on Selected Areas in Communications, vol. 19, no. 11, pp. 2254-2266, Nov. 2001.

[2] Z. Kostic, and N. Sollenberger, "Performance and implementation of dynamic frequency hopping in limited-bandwidth cellular systems", IEEE Transactions on Wireless Communications, vol. 1, no. 1, pp. 28-36, Jan. 2002.

[3] R. S. Karlsson, "Sharing radio resources in hierarchical cell structures utilizing slow frequency hopping", IEEE 49th Vehicular Technology Conference, vol. 1, pp. 412-416, 1999.

[4] K. S. Gilhousen, I. M. Jacobs, R. Padovani, Andrew J. Viterbi, Lindsay A. Weaver, and Charles E. Wheatley III, "On the capacity of a cellular CDMA system" IEEE Transactions on Vehicular Technology, vol. 40, no.2, pp. 303-312, May. 1991.

[5] S. Kishore, L. J. Greenstein, H. V. Poor, and S. C. Schwartz, "Capacity in a CDMA macrocell with a hotspot microcell: exact and approximate analyses", IEEE Vehicular Technology Conference, vol.2, pp. 1172 -1176, Fall 2001.

[6] S. Kishore, L. J. Greenstein, and S. C. Schwartz, "Uplink user capacity of a multi-cell CDMA system with hotspot microcells", IEEE Vehicular Technology Conference, vol. 2, pp. 992-996, Spring 2002.

Interference Analysis of TDD-CDMA Systems with Directional Antennas

Li-Chun Wang †, Shi-Yen Huang †, and Yu-Chee Tseng ‡
Department of Communication Engineering †
Department of Computer Science and Information Engineering ‡
National Chiao Tung University
†Email:lichun@cc.nctu.edu.tw

***Abstract*— This paper explores the advantages of using directional antennas in TDD-CDMA systems with asymmetric traffic. In the TDD-CDMA system, asymmetric traffic from neighboring cells may cause the cross-slot interference, which can seriously degrade system capacity. For TDD-CDMA systems with omni-directional antennas, many slot allocation algorithms have been proposed to avoid the cross-slot interference. These algorithms typically require a global control on the transmission direction (either downlink or uplink) in each time slot. Apparently, this requirement substantially limits the capability of TDD-CDMA systems to flexibly deliver asymmetric traffic services because every cell can have different traffic situations.**

We analyze the interference of the TDD-CDMA system with a tri-sector cellular architecture, where three diretional antennas are employed at each base station. We find that the directivity of directional antennas can provide an additional degree of freedom for allocating resources. This advantage enables the TDD-CDMA system to support asymmetric uplink and downlink traffic with different rates of asymmetry among neighboring cells in the entire system.

I. INTRODUCTION

CODE division multiple access (CDMA) systems comprise of two operation modes, namely frequency divison duplex (FDD) and time division duplex (TDD). In FDD-CDMA systems, a pair of frequency bands are used for uplink and downlink transmissions. In TDD-CDMA systems, the uplink and downlink transmissions are multiplexed into time slots on the same frequency band. The key advantage of the TDD-CDMA system is the capability to flexibly adjust uplink and downlink bandwidth by allocating different numbers of time slots [1]. Thus, compared to the FDD-CDMA system, the TDD-CDMA system is more suitable for applications with asymmetric traffic, such as Internet browsing, file transfer, etc.

However, asymmetric traffic from adjacent cells in the TDD-CDMA system may cause the *cross-slot interference*, which may seriously degrade system capacity. To support asymmetric traffic services in TDD-CDMA systems, we usually define the switching point as the boundary between uplink time slots and downlink time slots within a frame. If the two neighboring cells have different settings on their switching points due to different ratios of uplink and downlink traffic in each cell, then there exist some time slots that will be used for downlink transmissions in one cell, but for uplink transmissions in the neighboring cell. In this paper, we call this kind of interference due to opposite transmission directions as the *cross-slot interference*. Figure 1 illustrates an example when the cross-slot interference occurs in the TDD-CDMA system. In this example, time slot 3 is used for the uplink transmission in base station A, but it is used for the downlink transmission in base station B. Note that the transmission power of a base station is much higher than that of a mobile terminal. Thus, the cross-slot interference will seriously influence performance of the TDD-CDMA system.

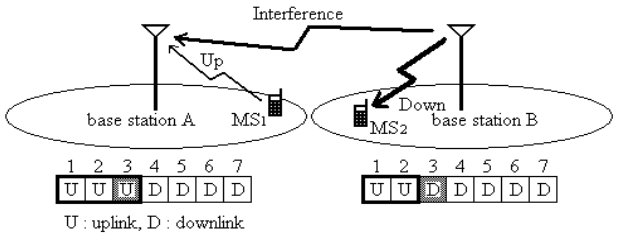

Fig. 1. An example of cross-slot interference. In this example, during slot 3, base station B causes the cross-slot interference to mobile station 1.

In the literature, interference analysis for TDD-CDMA systems has been reported in [2], [3]. In [2], the uplink interference, including the mobile-to-base and the base-to-base interference, was evaluated for the TDD-CDMA system with asymmetric traffic. It is concluded that the base-to-base interference will significantly decrease system capacity. In [3], the authors suggested to use a dynamic slot allocation scheme to avoid the interference in the TDD-

CDMA system. However, all the aforementioned works are concentrated on the TDD-CDMA system with omni-directional antennas employed at base stations.

To our knowledge, in the context of sectorized cellular structures, the interference issues in TDD-CDMA systems with asymmetric traffic, have not been fully addressed in the literature. In this paper, we develop an analyitical framework to evaluate the interference of the TDD-CDMA system with asymmetric traffic and directional antennas. By employing simple tri-sector base stations in the TDD-CDMA system, we find that the cross-slot interference can be restricted within a cell coverage area, thereby providing the flexibility of setting different switching points in all the neighboring cells. Our results indicate that by taking advantage of directivity of sector antennas, an interference-resolving algorithm can be developed for the TDD-CDMA system to support asymmetric traffic services with different downlink and uplink traffic ratio in every cell [4].

The rest of this paper is organized as follows. In Section II, we analyze the uplink interference. The downlink interference is analyzed in Section III. Numerical results are provided in Section IV. We give our concluding remarks in Section V.

II. Uplink Interference Analysis

Figure 2 shows the uplink interference scenario of the TDD-CDMA system. Without loss of generality, let's take sector S_{13} of cell 1 as an example. From the figure, one can find that there are four kinds of entities that will cause the uplink interference: (1) the mobile stations in the same sector of the serving base station, denoted as $I^{(u)}_{intra\_ms}$ in sector S_{13}; (2) the mobile stations in the different sector of the same cell, denoted as $I^{(u)}_{intra\_ms\_v}$ in sector S_{11}; (3) the mobile stations from the neighboring base station, denoted as $I^{(u)}_{inter\_ms}$ in sector S_{21}; (4) the base-to-base interference, denoted as $I^{(u)}_{inter\_bs}$ in the center of cell 2.

Assume that N mobile stations are uniformly distributed in each cell. Let p_{ms} be the received power at the base station after power control. Then the interference from the mobile stations of the same sector, i.e. sector S_{13}, can be expressed as follows

$$I^{(u)}_{intra\_ms} = \sum_{i=2}^{N/3} v_i \cdot p_{ms}, \tag{1}$$

where v_i is the activity factor.

Secondly, the interference from the mobile stations of

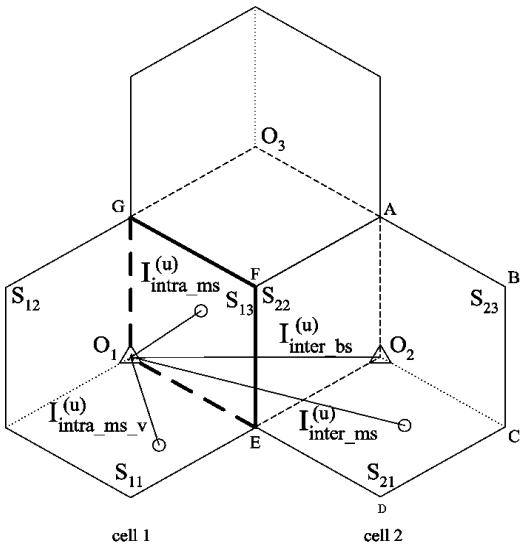

Fig. 2. Uplink interference scenario in the TDD-CDMA system.

sectors S_{11} and S_{12} can be written as

$$I^{(u)}_{intra\_ms\_v} = v\rho\, p_{ms} \sum_{\chi\in\{11,12\}} \int\int_{S_\chi} \frac{G_{13}(d_s,\theta_s)10^{\frac{\xi_s}{10}}}{G_\chi(d_s,\theta_s)10^{\frac{\xi_s}{10}}} \cdot \psi(G_{13}(d_s,\theta_s)10^{\frac{\xi_s}{10}}, G_\chi(d_s,\theta_s)10^{\frac{\xi_s}{10}})\, dxdy, \tag{2}$$

where $G_{13}(d_s,\theta_s)$ is the product of propagation loss and antenna gain for sector S_{13}; ξ_s is the shadowing component, characterized by a Gaussian random variable with zero mean and standard deviation of σ_s dB; v is defined in (1). We normalize the cell radius r_c to unity. Then the density of mobile stations in each cell is $\rho = \frac{\sqrt{3}N}{6}\ (\frac{\text{mobiles}}{\text{unit area}})$. Under the assumption of hard hand-off, $\psi(\cdot)$ indicates that the mobile terminal's transmission power is controlled by the base station whose pilot signal strength received by the mobile terminal is the highest.

$$\psi(\alpha,\beta) = \begin{cases} 1, & \text{if } \frac{\alpha}{\beta} \le 1 \\ 0, & \text{otherwise.} \end{cases} \tag{3}$$

In (2), $G_{13}(d_s,\theta_s)10^{\frac{\xi_s}{10}}$ represents the link gain, and $G_\chi(d_s,\theta_s)10^{\frac{\xi_s}{10}}$ represents the factor of power control to compensate for the link attenuation in sector S_χ, where $\chi \in \{11, 12\}$. For example, if $G_{13}(d_s,\theta_s)10^{\frac{\xi_s}{10}}$ is smaller than $G_{12}(d_s,\theta_s)10^{\frac{\xi_s}{10}}$, then the mobile terminal is served

by sector S_{12}, otherwise it will hand-off to sector S_{13}. By taking average with respect to v and ξ_s in (2), we obtain

$$E\left(I^{(u)}_{intra\_ms\_v}\right) = \rho\, p_{ms} E(v) \cdot \sum_{\chi\in\{11,12\}} \int\int_{S_\chi} \cdot \frac{G_{13}(d_s,\theta_s)}{G_\chi(d_s,\theta_s)}\, dxdy, \quad (4)$$

The interference from the mobile stations of cell 2, $I^{(u)}_{inter\_ms}$, can be written as[1]

$$I^{(u)}_{inter\_ms} = v\rho\, p_{ms} \sum_{\chi\in\{21,22,23\}} \int\int_{S_\chi} \frac{G_{13}(d_n,\theta_n)10^{\frac{\xi_n}{10}}}{G_\chi(d_s,\theta_s)10^{\frac{\xi_s}{10}}} \cdot \psi(G_{13}(d_n,\theta_n)10^{\frac{\xi_n}{10}}, G_\chi(d_s,\theta_s)10^{\frac{\xi_s}{10}})\, dxdy. \quad (5)$$

where ξ_s and ξ_n are Gaussian random variables with zero mean and standard deviation of σ_s and σ_n, respectively. Note that $\xi_n - \xi_s$ can be approximated by another normal distributed random variable with zero mean and a standard deviation of $\sqrt{\sigma_n^2+\sigma_s^2}$. Define $\eta = \frac{\ln 10}{10}$, and take average with respect to v, ξ_n, and ξ_s in (5). Then we have

$$E\left(I^{(u)}_{inter\_ms}\right) = \rho\, p_{ms} E(v) e^{\eta^2(\sigma_n^2+\sigma_s^2)/2} \cdot \sum_{\chi\in\{21,22,23\}} \int\int_{S_\chi} \frac{G_{13}(d_n,\theta_n)}{G_\chi(d_s,\theta_s)} \cdot \left[1 - Q\left(\frac{\ln\left(\frac{G_\chi(d_s,\theta_s)}{G_{13}(d_n,\theta_n)}\right)}{\eta\sqrt{\sigma_n^2+\sigma_s^2}} - \eta\sqrt{\sigma_n^2+\sigma_s^2}\right)\right] dxdy, \quad (6)$$

where $Q(x) = \frac{1}{\sqrt{2\pi}}\int_x^\infty e^{-t^2/2}dt$.

The base-to-base interference, $I^{(u)}_{inter\_bs}$, can be expressed as

$$I^{(u)}_{inter\_bs} = v\rho\, p_{bs} G_{13}(\theta_3) \cdot \sum_{\chi\in\{21,22,23\}} \int\int_{S_\chi} \frac{G_\chi(2r_c,\theta_s)10^{\frac{\xi_{bs}}{10}}}{G_\chi(d_s,\theta_s)10^{\frac{\xi_s}{10}}} \cdot \psi(G_{13}(d_n,\theta_n)10^{\frac{\xi_n}{10}}, G_\chi(d_s,\theta_s)10^{\frac{\xi_s}{10}})\, dxdy, \quad (7)$$

[1]Hereafter, the subscript s and n denote the variables associated with the serving cell and the neighboring cell, respectively. For example, ξ_n is the shadowing component of the neighboring cell, and ξ_s is the shadowing component of the serving cell.

where p_{bs} is the received power at the mobile terminal after power control, $G_{13}(\theta_3)$ is the receiver antenna gain, and ξ_{bs} is the shadowing component between the two base station with zero mean and a standard deviation of σ_{bs}. Note that σ_{bs} is smaller than σ_n and σ_s because σ_{bs} is to characterize the shadowing component of the transmission path between two base stations. Taking average over v, ξ_n, ξ_s, and ξ_{bs} in (7), we get

$$E\left(I^{(u)}_{inter\_bs}\right) = \rho\, p_{bs} E(v) e^{\eta^2(\sigma_s^2+\sigma_{bs}^2)/2} G_{13}(\theta_3) \cdot \sum_{\chi\in\{21,22,23\}} \int\int_{S_\chi} \frac{G_\chi(2r_c,\theta_x)}{G_\chi(d_s,\theta_s)} \cdot \Omega\left(\frac{G_\chi(d_s,\theta_s)}{G_{13}(d_n,\theta_n)}\right) dxdy, \quad (8)$$

where

$$\Omega\left(\frac{G_\chi(d_s,\theta_s)}{G_{13}(d_n,\theta_n)}\right) = \int_{-\infty}^{\infty} \frac{e^{-t^2}}{\sqrt{\pi}} \cdot Q\left(\sigma_s\eta + \frac{\sqrt{2}\sigma_n t - 10\log_{10}\left(\frac{G_\chi(d_s,\theta_s)}{G_{13}(d_n,\theta_n)}\right)}{\sigma_s}\right) dt. \quad (9)$$

To get the numerical results of (8), we can apply the Hermite polynomial method [5]. Recall that for the Hermite polynomial method,

$$\int_{-\infty}^{\infty} f(t)\exp(-t^2)\, dt = \sum_{i=1}^{k} w_i f(t_i) + R_k. \quad (10)$$

Hence, we can computed the $\Omega(\cdot)$ in (9) by substituting

$$f(t) = Q\left(\sigma_s\eta + \frac{\sqrt{2}\sigma_n t - 10\log_{10}\left(\frac{G_\chi(d_s,\theta_s)}{G_{13}(d_n,\theta_n)}\right)}{\sigma_s}\right) \quad (11)$$

into (10).

III. Downlink Interference Analysis

Now we analyze the downlink interference as shown in Fig. 3. We also focus on sector S_{13} of cell 1. From the figure, one can find that there are five kinds of interference sources: (1) the signals from the same antenna of the serving base station, denoted as $I^{(d)}_{intra\_bs}$ in sector S_{13}; (2) the signals from the neighboring sectors' antenna of the serving cell, denoted as $I^{(d)}_{intra\_bs\_v}$ in sector S_{11}; (3) the signals from the neighboring base station, denoted as $I^{(d)}_{inter\_bs}$ ic

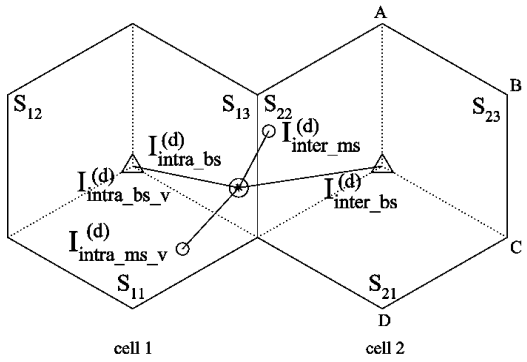

Fig. 3. Downlink interference scenario in the TDD-CDMA system.

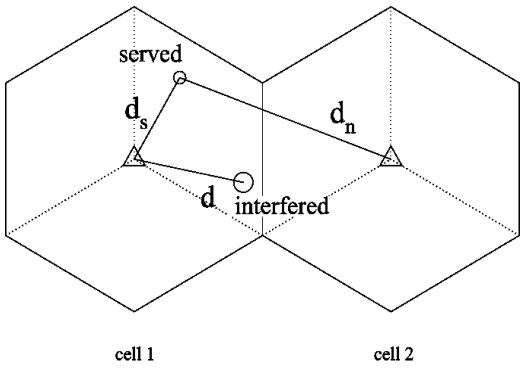

Fig. 4. Transmission path geometry.

cell 2; (4) the mobile stations from the neighboring sector of the serving cell, denoted as $I^{(d)}_{intra\_ms\_v}$ in sector S_{11}; (5) the mobile stations from other cells, denoted as $I^{(d)}_{inter\_ms}$ in sector S_{22}.

For the same antenna of the serving base station, we express $I^{(d)}_{intra\_bs}$ as

$$I^{(d)}_{intra\_bs} = v\rho\, p_{bs} \int\int_{S_{13}} \Phi_{S_{13}} \frac{G_{13}(d,\theta)10^{\frac{\xi_i}{10}}}{G_{13}(d_s,\theta_s)10^{\frac{\xi_s}{10}}} \cdot \psi(G_{22}(d_n,\theta_n)10^{\frac{\xi_n}{10}}, G_{13}(d_s,\theta_s)10^{\frac{\xi_s}{10}})\, dxdy, \tag{12}$$

where $\Phi_{S_{13}}$ is the orthogonal factor between the codes of the same sector, $0 \le \Phi_{S_{13}} \le 1$. In (12), as shown in Fig. 4, d and θ represent the distance and the angle of the interfered mobile terminal; d_s and d_n represent the distance to the serving cell and the neighboring cell, respectively. And ξ_i is the shadowing component between the base station and the interfered mobile terminal, which is a Gaussian random variable with zero mean and a standard deviation of σ_i. Taking average over v, ξ_n, ξ_s, and ξ_i, we can obtain

$$E\left(I^{(d)}_{intra\_bs}\right) = \rho\, p_{ms} E(v) e^{\eta^2(\sigma_s^2+\sigma_i^2)/2} \cdot \int\int_{S_\chi} \Phi_{S_{13}} \frac{G_{13}(d,\theta)}{G_{13}(d_s,\theta_s)} \Omega\left(\frac{G_{13}(d_s,\theta_s)}{G_{22}(d_n,\theta_n)}\right) dxdy, \tag{13}$$

where $\Omega(\cdot)$ is the same as in (9).

The interference from the neighboring sectors' antennas of the serving cell, $I^{(d)}_{intra\_bs\_v}$, can be expressed as

$$I^{(d)}_{intra\_bs\_v} = v\rho\, p_{bs} \sum_{\chi\in\{11,12\}} \int\int_{S_\chi} \frac{G_\chi(d,\theta)10^{\frac{\xi_i}{10}}}{G_\chi(d_s,\theta_s)10^{\frac{\xi_s}{10}}} \cdot \Phi_{S_\chi S_{13}} \psi(G_{13}(d_n,\theta_n)10^{\frac{\xi_n}{10}}, G_\chi(d_s,\theta_s)10^{\frac{\xi_s}{10}})\, dxdy. \tag{14}$$

Noteworthily, by taking advantage of the seperation of sector antennas, the orthogonality factor $\Phi_{S_\chi S_{13}}$ can be a non-zero value. By taking average with respect to v, ξ_n, ξ_s, and ξ_i, we get

$$E\left(I^{(d)}_{intra\_bs\_v}\right) = \rho\, p_{bs} E(v) e^{\eta^2(\sigma_s^2+\sigma_i^2)/2} \cdot \sum_{\chi\in\{11,12\}} \int\int_{S_\chi} \frac{G_\chi(d,\theta)}{G_\chi(d_s,\theta_s)} \cdot \Phi_{S_\chi S_{13}} \Omega\left(\frac{G_\chi(d_s,\theta_s)}{G_{13}(d_n,\theta_n)}\right) dxdy. \tag{15}$$

The downlink interference from the neighboring base station, $I^{(d)}_{inter\_bs}$, can be written as

$$I^{(d)}_{inter\_bs} = v\rho\, p_{bs} \sum_{\chi\in\{21,22,23\}} \int\int_{S_\chi} \frac{G_\chi(d,\theta)10^{\frac{\xi_i}{10}}}{G_\chi(d_s,\theta_s)10^{\frac{\xi_s}{10}}} \cdot \Phi_{S_\chi S_{13}} \psi(G_{13}(d_n,\theta_n)10^{\frac{\xi_n}{10}}, G_\chi(d_s,\theta_s)10^{\frac{\xi_s}{10}})\, dxdy. \tag{16}$$

Because the directivity of directional antennas, $\Phi_{S_{21}S_{13}}$ and $\Phi_{S_{23}S_{13}}$ can be non-zero values as in (14). However, $\Phi_{S_{22}S_{13}}$ should be as small as $\Phi_{S_{13}}$ in (12). By taking av-

erage with respect to v, ξ_n, ξ_s, and ξ_i, we obtain

$$E\left(I_{inter\_bs}^{(d)}\right) = \rho\, p_{bs} E(v) e^{\eta^2(\sigma_s^2+\sigma_i^2)/2} \cdot \sum_{\chi\in\{21,22,23\}} \int\int_{S_\chi} \frac{G_\chi(d,\theta)}{G_\chi(d_s,\theta_s)} \cdot \Phi_{S_\chi S_{13}} \Omega\left(\frac{G_\chi(d_s,\theta_s)}{G_{13}(d_n,\theta_n)}\right) dxdy. \quad (17)$$

where $\Omega(\cdot)$ is the same as (9).

For the downlink interference from the mobile stations of the neighboring sector, we express $I_{intra\_ms\_v}^{(d)}$ as

$$I_{intra\_ms\_v}^{(d)} = v\rho\, p_{ms} \sum_{\chi\in\{11,12\}} \int\int_{S_\chi} \frac{\left(d^{-4}\right) 10^{\frac{\xi_{ms}}{10}}}{G_\chi(d_s,\theta_s) 10^{\frac{\xi_s}{10}}} \cdot \psi(G_{13}(d_s,\theta_x)10^{\frac{\xi_s}{10}}, G_\chi(d_s,\theta_s)10^{\frac{\xi_s}{10}})\, dxdy. \quad (18)$$

where d is the distance between the interfering mobile terminal and the interfered mobile, and ξ_{ms} is the shadowing component between two mobile terminals. Taking average over v, ξ_s, and ξ_{ms}, we obtain

$$E\left(I_{intra\_ms\_v}^{(d)}\right) = \rho\, p_{ms} E(v) e^{\eta^2(\sigma_s^2+\sigma_{ms}^2)/2} \cdot \sum_{\chi\in\{11,12\}} \int\int_{S_\chi} \frac{\left(d^{-4}\right)}{G_\chi(d_s,\theta_s)}\, dxdy. \quad (19)$$

For the interference from mobile stations of the other cell, $I_{inter\_ms}^{(d)}$, we can express it as

$$I_{inter\_ms}^{(d)} = v\rho\, p_{ms} \sum_{\chi\in\{21,22,23\}} \int\int_{S_\chi} \frac{\left(d^{-4}\right) 10^{\frac{\xi_{ms}}{10}}}{G_\chi(d_s,\theta_s) 10^{\frac{\xi_s}{10}}} \cdot \psi(G_{13}(d_n,\theta_n)10^{\frac{\xi_n}{10}}, G_\chi(d_s,\theta_s)10^{\frac{\xi_s}{10}})\, dxdy. \quad (20)$$

Taking average over v, ξ_n, ξ_s, and ξ_i, we obtain

$$E\left(I_{inter\_ms}^{(d)}\right) = \rho\, p_{ms} E(v) e^{\eta^2(\sigma_s^2+\sigma_{ms}^2)/2} \cdot \sum_{\chi\in\{21,22,23\}} \int\int_{S_\chi} \frac{\left(d^{-4}\right)}{G_\chi(d_s,\theta_s)} \Omega\left(\frac{G_\chi(d_s,\theta_s)}{G_{13}(d_n,\theta_n)}\right) dxdy. \quad (21)$$

Note that (13), (17), and (21) can be computed based on the Hermite polynomial approach introduced in (10).

IV. Numerical Results

In this section, we give some numerical results based on the interference analysis in Sections III and IV. Consider the interference scenario as shown in Fig. 2. Let $\sigma_s = 9$ dB, $\sigma_n = 8$ dB, and $\sigma_{bs} = 3$ dB. The center of cell 1 is set at $(0, 0)$. Let r_c be one kilometer, and the center of cell 2 is at $(2\text{ km}, 0)$. We calculate the interference of the TDD-CDMA system for the cases with omni-directional antennas and directional antennas.

Figure 5 shows the base-to-base interference for the TDD-CDMA system with directional antennas. In this figure, points A, B, C, and D stand for the corners of cell 2 in Fig. 2. According to (8), the base-to-base interference is calculated when a mobile moves to different locations within cell 2. The values in the z-axis represent the base-to-base interference levels normalized to p_{bs} received at cell 1. One can see that as a mobile terminal is located at point A of cell 2, the base station of cell 1 will receive the strongest base-to-base interference from cell 2. On the other hand, if a user in cell 2 is located at points B, C, or D, the base-to-base intererence from cell 2 to cell 1 is negligible. By using directional antennas, the strong base-to-base interference is restricted in the area of hexagon labeled with A-O_2-E-O_1-G-O_3 as shown in Fig. 2. Hence, the base-to-base interference can be possibily avoided by coordinating the switching points of only three sectors in the TDD-CDMA system with the tri-sector cellular structure.

For comparison, Fig. 6 shows the base-to-base interference for the TDD-CDMA system with omni-directional antennas. One can find that cell 1 receives strong base-to-base interference from cell 2 regardless of the mobile locations in cell 2. Thus, the base-to-base interference for the TDD-CDMA system with omni-directional antennas will influence all the surrounding cells, thereby requiring the global control on the design of switching points within the entire network.

To verify our analysis , Table I shows the results obtained from both analysis and simulation. Based on the Hermite polynomial approach, (6) and (8) can accurately estimate the interference in the TDD-CDMA system compared to simulations. Noteworthily, the base-to-base interference is higher than the interference from mobile terminals because the transmission power of a base station is greater than that of a mobile station.

In Table II, we show the analytical and simulation results for downlink interference. The analysis results are obtained by evaluating (17) and (21). Assume the interfered mobile terminal be located at $(0.4\text{ km}, 0)$. Let σ_i be 8.5 dB, and σ_{ms} be 10 dB. One can see that $I_{inter\_ms}^{(d)}$ is higher than $I_{inter\_bs}^{(d)}$ because mobile terminals close to cell boundary will introduce a large cross-slot interference on the serving

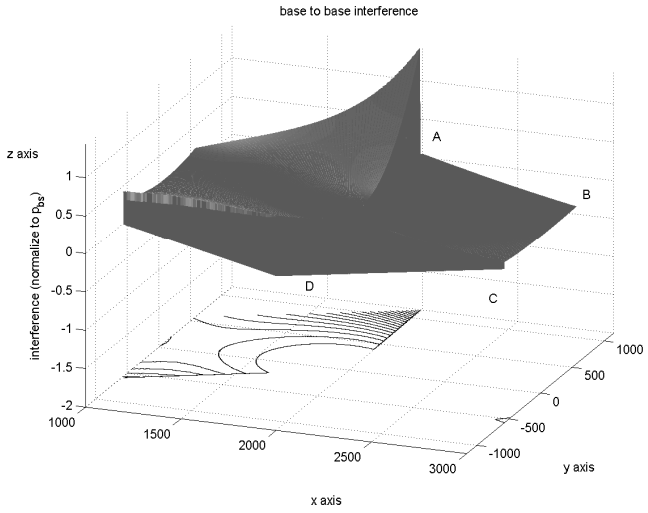

Fig. 5. Uplink base-to-base interference from cell 2 to cell 1. (directional antenna)

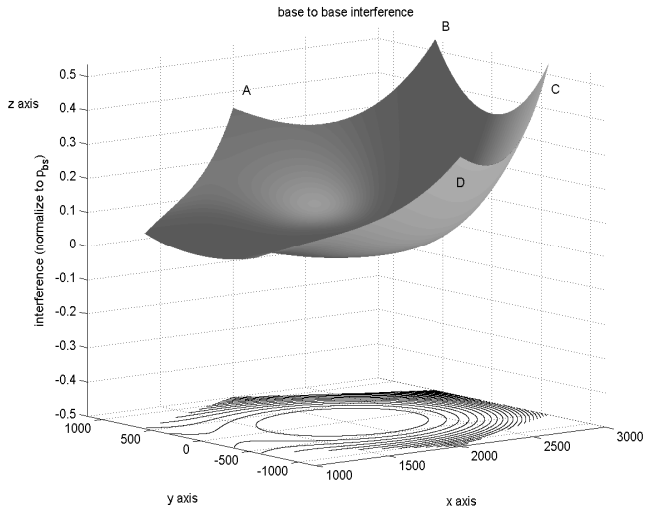

Fig. 6. Uplink base-to-base interference from cell 2 to cell 1. (omni-directional antenna)

mobile due to a short distance. By coordinating the switching points of the three adjacent sectors belowing to three different base stations, we can avoid the mobile-to-mobile cross-slot interference for the TDD-CDMA system.

V. Conclusion

In this paper, we have developed an analytic framework to evaluate the interference of the TDD-CDMA system with directional antennas. Our results imply that the strong base-to-base interference will be restricted into a small area. Thus, by coordinating the setting of only three sectors, the TDD-CDMA system with directional antennas can allocate uplink/downlink bandwidth more flexibly than a system with omni-directional antennas.

TABLE I

Comparison of uplink interference based on analysis and simulation.

$I^{(u)}_{inter\_ms}$	Simulation	7.0999 (p_{ms})
	Analysis	6.9223 (p_{ms})
	Inaccuracy	2.5652%
$I^{(u)}_{inter\_bs}$	Simulation	7.6744 (p_{bs})
	Analysis	7.4540 (p_{bs})
	Inaccuracy	2.9571%

TABLE II

Comparison of downlink interference based on analysis and simulation.

$I^{(d)}_{inter\_ms}$	Simulation	158.1143 (p_{ms})
	Analysis	148.7765 (p_{ms})
	Inaccuracy	6.2764%
$I^{(d)}_{inter\_bs}$	Simulation	30.5988 (p_{bs})
	Analysis	28.9837 (p_{bs})
	Inaccuracy	5.5726%

References

[1] M. Haardt, A. Kleig, R. Koehn, M. Purat, V. Sommer, and T. Ulrich, "The TD-CDMA based TRRA TDD mode," IEEE Journal on Selected Areas in Communications vol. 18, no. 8, pp. 1375-1385, Aug. 2000

[2] Xingyao Wu, Lie-Liang Yang and Lajos Hanzo, "Uplink capacity investigations of TDD-CDMA," IEEE Vehicular Technology Conference, pp. 997-1001, Spring 2002.

[3] H. Holma, S. Heikkinen, O.-A. Lehtinen, A. Toskala, "Interference considerations for the time division duplex mode of the UMTS terrestrial radio access," IEEE Journal on Selected Areas in Communications, vol. 18, no. 8, pp. 1386-1393, Aug. 2000

[4] Li-Chun Wang, Shi-Ye Huang, and Yu-Chee Tseng, "A novel interference-resolving algorithm to support asymmetric services in TDD-CDMA systems with directional antennas," IEEE Vehicular Technology Conference, pp. 327 -330, Spring 2002.

[5] L. Jean-Paul, *Narrowband Land-Mobile Radio Networks*, pp. 325 -326, Artech House, 1993.

An Analytical Framework for Capacity and Fairness Evaluation in High Speed Wireless Data Networks

Chiung-Jang Chen* and Li-Chun Wang†
National Chiao Tung University, Taiwan, R.O.C.
*Email : cjch.cm90g@nctu.edu.tw, †Email : lichun@cc.nctu.edu.tw

***Abstract*— This paper presents an analytical framework to evaluate the downlink capacity and fairness performance for high speed wireless data networks from both the physical layer and the network layer perspectives. From the physical layer standpoint, we take into account of propagation loss, log-normal shadowing and Nakagami fading. From the network layer perspective, we model different scheduling policies and the impact of nonuniform traffic intensity of mobile users into our framework. We analyze the joint effects of radio channel impairments, nonuniform traffic intensity and scheduling algorithms on the downlink capacity and fairness performance of wireless data networks based on the developed framework. Our results suggest that it is crucial for wireless scheduling algorithms to consider not only the radio channel impairments, but also the traffic intensity distribution in the whole network.**

I. Introduction

The demand of delivering the Internet services in the wireless network is driving the direction of technology evolution. An obvious influence of the Internet on the wireless industry is the trend to enhance downlink capacity because the traffic volume of wireless Internet services in the downlink is expected to be much higher than that in the uplink. The focus of this paper is to propose an analytical approach to evaluate the capacity and fairness performance of the system that uses the shared channel in high speed downlink transmissions.

Many current industrial standards such as IS-856 [1] and 3GPP R5 [2] have adopted scheduling technologies combined with adaptive modulation for high data rate downlink transmissions in a shared channel. By adopting scheduling policy in a shared channel, a base station can allocate its resource, e.g. power, to the user with better channel quality, while postponing the transmissions of users with poor channel quality. Combined with adaptive modulation/coding techniques, packet scheduling algorithms can exploit the variation of the time-varying channels among users to achieve higher spectral efficiency [3].

The literature survey on wireless scheduling technologies is summarized as follows. Some previous works, such as [4], [5], [6], proposed variety of wireless scheduling algorithms subject to different QoS constrains. In [4], [5], the authors extended the fair scheduling policies for a wired channel to scheduling algorithms for a wireless channel. However, they adopted a simple two-state channel model, which may not be able to fully characterize the radio channel impairments. In [6], the authors presented an optimum packet scheduler under the long-term fairness requirement among users. By simulation, the authors demonstrated that their proposed scheduler can improve capacity compared with the round-robin scheduling scheme. In addition, some papers in [7], [8], [9] investigated how to combine other techniques with schedulers to improve the downlink performance of the wireless data networks. In [7], the authors proposed to amplify the multiuser diversity gain by transmitting the signal through multiple antennas with randomly varying magnitude and phase. However, the impact of propagation loss and shadowing was not addressed in [7]. The authors of [8] demonstrated that one-by-one time division scheduling scheme in the downlink DS-CDMA can provide better energy efficiency. In [9], the simulation performance of applying open loop and closed loop transmit diversity techniques combined with schedulers was studied in wireless packet data systems.

To our knowledge, a generic analytical framework to evaluate different scheduling policies subject to the impact of radio channel impairments is lacking in the literature. Generally speaking, there exists a dilemma of achieving better system capacity and maintaining fairness among the users in a resource-sharing environment. The challenge for wireless scheduling techniques is to capture the characteristics of fast varying wireless channels into the scheduling algorithms. In this paper, we will present an analytical framework to investigate the downlink capacity and fairness performance of wireless data networks from both the physical and network layer perspectives. Our model takes into

account of radio channel impairments including path loss, shadowing and fading. Furthermore, we model the effects of nonuniform traffic intensity and scheduling policies into our framework. This analytical framework is aimed to analyze the joint effects of radio channel impairments and scheduling policies on the downlink capacity and fairness performance in wireless data networks.

The rest of this paper is organized as follows. In Section II, we describe our system model including the radio channel model and traffic queueing model. In Section III, we derive the performance metrics under different scheduling disciplines. In Section IV, we give some numerical results based on our developed model. In Section V, we provide our concluding remarks.

II. System Model

We consider a single-cell system as shown in Fig. 1. Two mobile users (denoted as users 1 and 2) are located in the cell with a distance of r_1 and r_2 to the serving base station, respectively. Without loss of generality, we assume that user 1 is closer to the base station than user 2, i.e. $r_2 \geq r_1$.

A. Radio Channel Model

We assume the radio link is subject to propagation loss, slow-varying log-normal distributed shadowing and fast-varying Nakagami fading. Thus, the composite distribution of the link gain G has the following probability density function

$$f_G(g) = \int_0^\infty \left(\frac{m}{\Omega}\right)^m \frac{g^{m-1}}{\Gamma(m)} \exp\left(-\frac{mg}{\Omega}\right) \times \frac{\xi}{\sqrt{2\pi}\sigma\Omega} \exp\left(-\frac{(10\log_{10}\Omega - \eta)^2}{2\sigma^2}\right) d\Omega \ , \quad (1)$$

where

η	$= -10\alpha\log_{10}(r) - L_0$;
r	distance between transmitter and receiver in km;
α	path loss exponent;
σ	shadowing standard deviation;
L_0	path loss at the distance of 1 km;
m	Nakagami fading parameter;
ξ	$= 10/\ln(10)$.

According to [10], the composite Gamma-log-normal distribution can be approximated by another log-normal distribution with the following modified mean η_G and variance σ_G^2. That is,

$$\eta_G = \mathrm{E}\left[G_{[dB]}\right] = -10\alpha\log_{10}(r) - L_0 + A(m) \quad (2)$$

and

$$\sigma_G^2 = \mathrm{Var}\left[G_{[dB]}\right] = \sigma^2 + B(m) \quad (3)$$

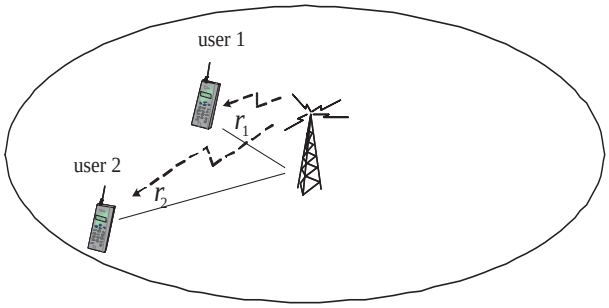

Fig. 1. The system model where two users are located at the distance r_1 and r_2 away from the base station.

where $A(m)$ and $B(m)$ are the constants related to the Nakagami parameter m. For Rayleigh fading, i.e. $m = 1$, we can obtain $A = -2.5$ and $B = 31$. For the fading channel containing a line-of-sight (LOS) component, e.g. $m = 8$, we have $A = -0.28$ and $B = 2.5$.

Let P_t denote the transmitting power of the base station and N_0 denote the thermal noise power. Then the received signal to noise ratio (SNR) at the ith mobile user is

$$\gamma_i(r_i) = P_t G(r_i)/N_0 \ . \quad (4)$$

Combining equations (1) to (4), we can model the ith user's received SNR γ_i as a log-normal distribution with the following mean and variance:

$$\eta_{\gamma_i} = -10\alpha\log_{10}(r_i) - L_0 + A(m) + 10\log_{10}(Pt/N_0) \quad (5)$$

and

$$\sigma_{\gamma_i}^2 = \sigma_i^2 + B(m) \ . \quad (6)$$

Assume an adaptive M-ary QAM modulation is adopted in downlink transmissions when the channel condition is good. Thus, it is expected that the achievable throughput is proportional to the received SNR. From [11], the delivered throughput from the base station to user i is expressed as

$$T_i(\gamma_i) = \log_2(1 + c\gamma_i) \ , \quad (7)$$

where $c = -1.5/\ln(5 \cdot \mathrm{BER})$ is the constant subject to the bit error rate (BER) requirement.

B. Traffic Queueing Model

Now we apply a two-dimensional birth-and-death Markov model to incorporate the effects of different traffic intensity in each user and different scheduling policies at the base station. We consider a time-slotted system. The packet arrivals of users 1 and 2 are generated by independent Poisson distribution with the average arrival rates λ_1 and λ_2, respectively. Assume the received SNR by each user is correctly and immediately sent back to the base station, as shown in Fig. 2. Then the base station decides to transmit one packet to user 1 or 2 with full power P_t in each time slot.

Let (i, j) denote a system state with i packets in the queue of user 1 and j packets in the queue of user 2. Then the state space can be written as

$$S = \{ (i,j) \,|\, 0 \le i \le K_1, 0 \le j \le K_2 \} \ , \qquad (8)$$

where K_1 and K_2 denote the queue size of users 1 and 2, respectively. The processing time of one packet at the base station is assumed to be an exponential distribution with mean service time $1/\mu$. Since the downlink transmission of the base station is shared by these two users in a time division manner, the mean service time for individual user is reduced. Let $1/\beta_{ij}$ and $1/\delta_{ij}$ denote the mean service time of users 1 and 2 at state (i, j), respectively. Thus, we can have

$$\mu = \beta_{ij} + \delta_{ij} \ . \qquad (9)$$

If the system is in equilibrium, the whole process can be modelled as a two-dimensional birth-and-death Markov chain as shown in Fig. 3. To model the effect of scheduling policies, we assume the effective service rate for each user is proportional to the probability of that user being served. Let f_{ij} denote the probability that user 1 is served at state (i, j). Then

$$\beta_{ij} = f_{ij}\mu \ , \qquad (10)$$

and

$$\delta_{ij} = (1 - f_{ij})\mu \ . \qquad (11)$$

Referring to Fig. 3, we can obtain the global balance equation [12] for each state (i, j) as

$$\begin{aligned}(\beta_{ij} + \delta_{ij} + \lambda_1 + \lambda_2)\pi_{ij} &= \lambda_1\pi_{i-1,j} \\ &+\lambda_2\pi_{i,j-1} + \beta_{i+1,j}\pi_{i+1,j} + \delta_{i,j+1}\pi_{i,j+1} \ , \end{aligned} \qquad (12)$$

where π_{ij} is the steady state probability. In addition, the state probabilities π_{ij} have to satisfy the condition

$$\sum_{(i,j)\in S} \pi_{ij} = 1 \ . \qquad (13)$$

In general, it is difficult to get the closed-form expression for π_{ij}. However, it can be solved numerically via the global balance equation in (12) and the normalization condition in (13). Note that in (10) and (11), f_{ij} is the probability of user 1 being served, which is determined according to scheduling strategies.

C. Fairness and Capacity

One of the goals in this paper is to evaluate the fairness and capacity of a high speed wireless data network with consideration of radio channel impairments. To begin with, we define F_i as the average probability of user i being served. F_i can be obtained by summing f_{ij} over all the possible states. That is,

$$F_1 = \sum_{i=1}^{K_1}\sum_{j=0}^{K_2} \pi_{ij} f_{ij} \ , \qquad (14)$$

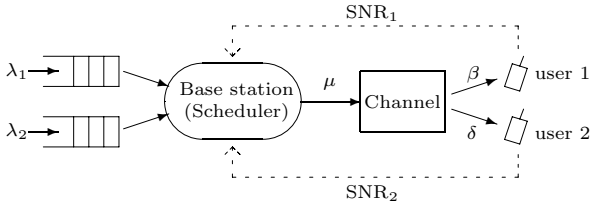

Fig. 2. The block diagram to illustrate the operation of a wireless data network.

and

$$F_2 = \sum_{j=1}^{K_2}\sum_{i=0}^{K_1} \pi_{ij}(1 - f_{ij}) \ . \qquad (15)$$

where K_1 and K_2 are the queue size of users 1 and 2, respectively. In terms of F_1 and F_2, we can further assess the fairness performance between the two users by defining an indicator, i.e.

$$F = F_1/F_2 \ . \qquad (16)$$

Obviously, $F > 1$ means that user 1 gets more chances to receive packets from the serving base station or vice versa.

On the other hand, we define the capacity as the average delivered throughput in equilibrium. For an individual user, the capacity of user i can be written as

$$\begin{aligned} E[T_1] \quad = \quad & \sum_{i=1}^{K_1}\sum_{j=0}^{K_2} \pi_{ij} f_{ij} E[T_1 | \text{user 1} \\ & \text{is served at state } (i,j)] \end{aligned} \qquad (17)$$

and

$$\begin{aligned} E[T_2] \quad = \quad & \sum_{j=1}^{K_2}\sum_{i=0}^{K_1} \pi_{ij}(1 - f_{ij}) E[T_2 | \\ & \text{user 2 is served at state } (i,j)] \ , \end{aligned} \qquad (18)$$

where T_i is the delivered throughput from the serving base station to user i, which was defined in (7). Finally the total system capacity is defined as the sum of the delivered throughput to each user from the base station, i.e.

$$T_{tot} = E[T_1] + E[T_2] \ . \qquad (19)$$

III. Scheduling Policy

In the previous section, we have developed a Markov model to represent the operation of a wireless data network. Recall that in the proposed model, the effective service rate to individual user is proportional to f_{ij}, i.e. the probability of user i being served. In the following, we will explain how to determine f_{ij} based on three schedulers considered: the random scheduler (RS), the greedy scheduler (GS) and the queue-length based proportional fairness scheduler (QS).

A. Random Scheduler

The random scheduler (RS) assigns time slots to users in a pseudo random manner. Thus, in the case with two users, we have

$$f_{ij} = 1/2 \quad \text{for all } (i,j) \in S^- \ , \tag{20}$$

where $S^- = \{(i,j)|1 \le i \le K_1, 1 \le j \le K_2\}$ is the subset of S containing all the states with more than one packet in both queues. When one of the queues is empty and the other is not, we assume the user in the queue will be definitely served. Clearly, the main advantage of the RS method is that it is unbiased to any mobile users. However, because neglecting the link condition in mobile users, the RS method may miss some chances to deliver more throughput to the user with good channel quality. Therefore, the RS method has worse capacity performance compared with other schedulers.

B. Greedy Scheduler

By contrast, the greedy scheduler (GS) always pursues the maximum system capacity by assigning time slots to the user with the best SNR. Capacity improvement of the GS is achieved at the expense of sacrificing the fairness among users. Based on the GS policy, f_{ij} can be written as

$$f_{ij} = \Pr\{\gamma_1 > \gamma_2\} \quad \text{for all } (i,j) \in S^- \ , \tag{21}$$

where γ_i is the SNR of user i and S^- is defined as in (20).

Substituting (5) and (6) into (21) and assuming γ_1 and γ_2 are independent, we can simplify f_{ij} as

$$f_{ij} = Q\left(-\frac{10\alpha}{\sigma}\log_{10}(d)\right) \ , \tag{22}$$

where $Q(x) = \int_x^\infty \frac{1}{\sqrt{2\pi}} e^{-t^2/2} dt$, α is the path loss exponent, $d = r_2/r_1$ and $\sigma = \sqrt{\sigma_1^2 + \sigma_2^2 + 2B(m)}$. Here σ_1 and σ_2 are the log-normal shadowing standard deviations of users 1 and 2, respectively; $B(m)$ is defined as in (3).

C. Queue-Length Based Proportional Fair Scheduler

Unlike the GS policy that places emphasis on the radio channel condition only, we propose a queue-length based proportional fair scheduler (QS) that takes into account of both radio link impairments and the waiting queue behavior in the base station. According to the proposed QS, not only the user with better link quality has a higher priority, but also the user who has longer length in the waiting queue can increase his priority. Specifically, for the GS policy,

$$f_{ij} = \Pr\left\{\frac{\gamma_1}{\gamma_2} > \left(\frac{j}{i}\right)^\kappa\right\} \quad \text{for all } (i,j) \in S^- \ , \tag{23}$$

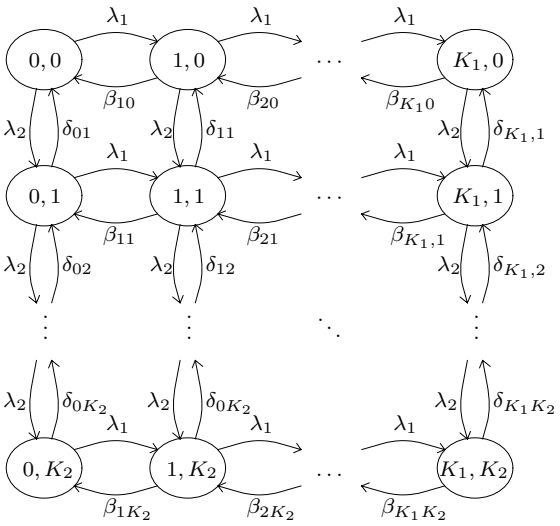

Fig. 3. Markov chain representation of the wirelss data network with two users.

where $\kappa \ge 0$ is an empirical constant used to raise the priority of user 2. When the waiting queue length of user 2, e.g. $j = 2$, is larger than that of user 1, e.g. $i = 1$, the SNR of user 1 has to be 2^κ times stronger than that of user 2 for user 1 to get services from the base station. The QS becomes the same as the GS if $\kappa = 0$. In other word, the QS provides a mechanism to balance between the system capacity and fairness. Using the similar way to get (22), we combine (5), (6) and (23) to obtain

$$f_{ij} = Q\left(-\frac{10}{\sigma}\log_{10}\left\{\left(\frac{i}{j}\right)^\kappa d^\alpha\right\}\right) \ . \tag{24}$$

IV. Numerical Results

In this section, we apply the proposed analytical framework to give some numerical examples to illustrate the effects of user's locations, nonuniform traffic intensity and radio channel impairments on the downlink capacity and fairness issue in wireless data networks. The following parameter values are used for numerical evaluation: $P_t = 40$ dBm, $L_0 = 128$ dBm, $N_0 = -100$ dBm, $\alpha = 4$, $\sigma_1 = \sigma_2 = 8$, $\kappa = 20$, and $K_1 = K_2 = 10$.

Figure 4 illustrates the effect of user's locations on the capacity and fairness of a wireless data networks with different scheduling policies. We set $\lambda_1/\mu = \lambda_2/\mu = 1.25$. In this example, the location of user 1 is fixed at $r_1 = 0.3$ km away from the base station, while user 2 varies its location from r_1 to $6r_1$ for investigating the impact caused by different near-far conditions. In the figure, we denote $d = r_2/r_1$. From Figs. 4-(a) and 4-(b), one can see that the GS has the greatest capacity advantage at the cost of sacrificing fairness for the farther user, i.e. user 2 in this example. On the contrary, the RS is the fairest scheduler for any value of d, but

has the worst capacity. As for the QS, it significantly improves the unfairness when compared with the RS but without losing too much capacity when compared with the GS. Therefore, it indicates that the QS can achieve both high capacity and fairness for a wireless data network without the impact of the near-far effect among users.

Figures 5-(a) and 5-(b) show the fairness with respect to each user. They can be used to elaborate the dynamics behind Fig. 4. From Fig. 5, one can observe that for GS and QS, user 1 has larger probability to obtain the packet transmission than user 2 when $d \geq 2$. Moreover, a user closer to the base station is capable of receiving higher data rates thanks to adaptive modulation. As long as this user has high traffic demand for downlink transmission, a large difference of achievable throughput between the near and far users occurs for the GS and QS as shown in the next Fig. 6.

Figs. 6-(a) and 6-(b) show the capacity of users 1 and 2 for different scheduling policies with different near-far conditions among users. When $d \geq 2$, the system capacity is used mainly by user 1. This observation can also explain why the system capacity in Fig. 4-(b) is less sensitive to the location of user 2 for both GS and QS. Consequently, it is concluded that the capacity obtained by applying the RS becomes much worse if the users are densely located in the cell fringe.

Figure 7 demonstrates the effect of nonuniform traffic intensity among mobile users on the system performance in terms of capacity and fairness. In this example, we keep the total traffic intensity $(\lambda_1 + \lambda_2)/\mu = 2.5$, but vary the ratio λ_2/λ_1. The locations of both users are fixed and $r_2/r_1 = 3$. It is indicated that a farther user with heavier traffic intensity eases the unfairness phenomenon caused by different distances from users to the base station. The improvement of unfairness is particularly significant for the GS. At the same time, the capacity obtained by using the GS and QS decreases as λ_2/λ_1 increases. These observations will be explained shortly in Fig. 8.

Figure 8 shows the impact of nonuniform traffic on the fairness and capacity for users 1 and 2 with different scheduling policies. From Figs. 8-(a) and 8-(b), a user with heavier traffic intensity can have higher probability of being served because the heavier traffic intensity can increase the utilization of the base station. The decrease of F_1 and the increase of F_2 lead to the decrease of T_1 in Fig. 8-(c) and the increase of T_2 in Fig. 8-(d), respectively. Because transmitting one packet to the closer user usually results in higher capacity than to the farther user, the combined effect by the decrease of T_1 and the increase of T_2 is a decrease of the system capacity as shown in Fig. 7-(b).

Figure 9 illustrates the impact of radio channel impairments on the system performance in terms of fairness and capacity for wireless data networks with different scheduling policies. We take the curve with $\sigma_1 = \sigma_2 = 8$ and $m = 1$ as the baseline. When the Nakagami parameter m is changed to, e.g. $m = 8$, a fading environment with a strong LOS component, it is interesting to note that both the capacity and fairness performance degrade for the QS and RS. In the LOS environment, radio channels have more specular components than Rayleigh fading so that the SNR of the farther user has a less chance to exceed that of the closer user. Hence, the bias against user 2 becomes more apparent, thereby leading to worse fairness performance. Furthermore, in a channel with strong LOS components, the probability that a user is served at the higher peaks of the radio channel is also reduced. As a result, the system capacity is reduced with a large m. We also investigate the impact of shadowing with $\sigma_1 = \sigma_2 = 6$. As indicated in the figure, by reducing the shadowing standard deviation, the performance becomes worse from both aspects of capacity and fairness. These phenomena can also be explained by the same arguments as the previous case of LOS components.

V. Conclusions

In this paper, we have developed an analytical framework to investigate the capacity and fairness in wireless data networks. The proposed generic analytical framework can integrate radio channel impairments, nonuniform traffic intensity and scheduling polices into an unified model. From the physical layer perspective, this analytical framework incorporates the radio channel impairments including Nakagami fading, shadowing and path loss. From the network layer perspective, our framework can model different scheduling polices, including the random scheduler (RS), the greedy scheduler (GS), and the queue-length based proportional fair scheduler (QS). Based on the results obtained by applying our proposed framework, some important conclusions can be drawn as follows:

- When all the users in a cell have uniform and high traffic intensity, the system capacity is used mainly by those users who are close to the serving base station. Under such a circumstance, if the users are located on the cell fringe, applying the RS policy may have a significant capacity loss compared with the GS and QS.
- If the users in a cell have nonuniform traffic intensity, the users close to the base station with high traffic intensity dominate the system capacity. In a scenario where the traffic intensity concentrates on a hot spot located in the cell border, the system capacity is reduced for both the GS and QS methods.
- Radio link fluctuations induced by Nakagami fading as well as log-normal shadowing can improve both system capacity and fairness performance in the case of multiple users of which radio link conditions are uncorrelated. System operators can

take advantage of this characteristics to deploy high speed wireless data network more efficiently.

In summary, our results suggest that it is crucial for wireless scheduling technologies to consider not only the radio channel impairments, but also the traffic intensity distribution in the whole network.

References

[1] TIA/EIA IS-856, "cdma2000: High rate packet data air interface specification".

[2] 3GPP TR25.950, "UTRA High Speed Downlink Packet Access".

[3] Paul Bender et al, "CDMA/HDR: A bandwidth-efficient high-speed wireless data service for nomadic users," *IEEE Communications Magazine*, pp. 70-77, July, 2000.

[4] S. Lu, V. Bharghavan, and R. Srikant, "Fair scheduling in wireless packet networks," *IEEE INFOCOM'98*, vol. 3, pp. 1108-1111, 1998.

[5] T. Ng, I. Stoica, and H. Zhang, "Packet fair queueing algorithms for wireless networks with location-dependent errors," *IEEE/ACM Trans. on Networking*, vol. 7, pp. 473-489, Aug., 1999.

[6] Xin Liu, E. K. P. Chong and N. B. Shroff, "Opportunistic transmission scheduling with resource-sharing constrains in wireless networks," IEEE *IEEE J. Select. Areas Commun.*, vol. 19, no. 10, pp. 2053-2064, Oct., 2001.

[7] P. Viswanath, David N. C. Tse, and R. Laroia, "Opportunistic beamforming using dumb antennas," *IEEE Trans. on Information Theory*, vol. 48, pp. 1277-1294, Jun., 2002.

[8] F. Berggren, S. L. Kim, R. Jantti and J. Zander, "Joint power control and intracell scheduling of DS-CDMA nonreal time data," *IEEE J. Select. Areas Commun.*, vol. 19, pp. 1860-1870, Oct., 2001.

[9] A. G. Kogiantis, N. Joshi and O. Sunay, "On transmit diversity and scheduling in wirelees packet data," *IEEE Proc. ICC*, vol. 8, pp. 2433-2437, 2001.

[10] G. J. Stuber, *Principles of Mobile Communication,* Kluwer, 1996.

[11] X. Qiu and K. Chawla, "On the performance of adaptive modulation in cellular systems," *IEEE Trans. on Communications*, vol. 47, no. 6, pp. 884-895, Jun., 1999.

[12] L. Kleinrock, *Queueing Systems,* John Wiley, 1975.

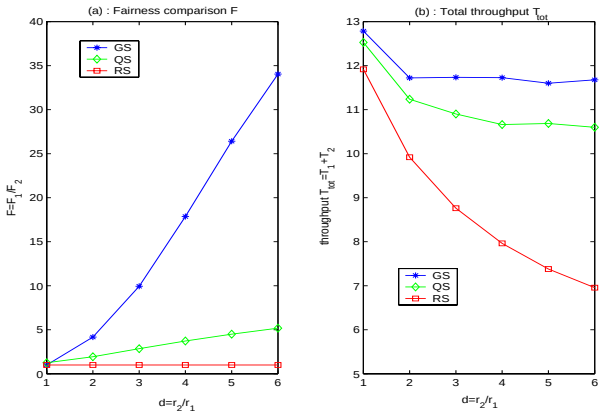

Fig. 4. Effect of user's locations on fairness and capacity of a wireless data network. Here, GS: greedy scheduler; QS: queue-length based proportional fair scheduler; RS: random scheduler.

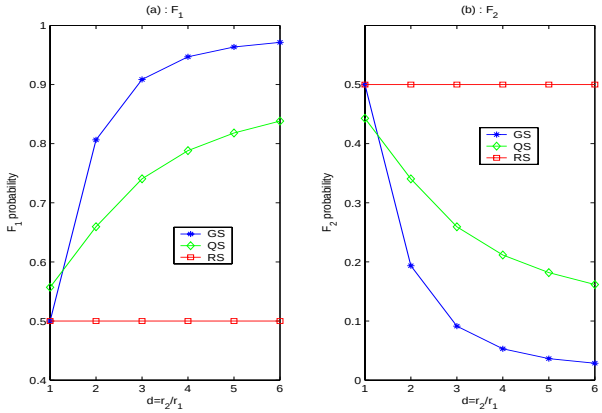

Fig. 5. Probability of getting services for users 1 and 2 for different scheduling policies under different near-far conditions among users. Here, GS: greedy scheduler; QS: queue-length based proportional fair scheduler; RS: random scheduler.

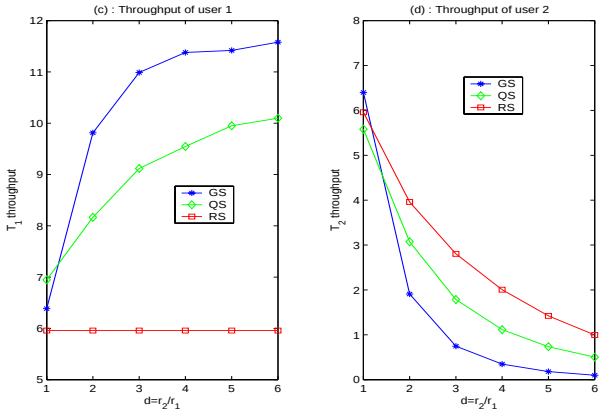

Fig. 6. Achievable capacity for users 1 and 2. Here, GS: greedy scheduler; QS: queue-length based proportional fair scheduler; RS: random scheduler.

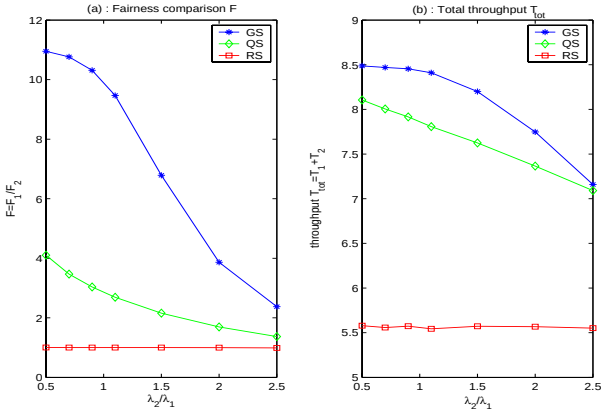

Fig. 7. Effect of user's nonuniform traffic intensity on the system performance in terms of fairness and capacity for different scheduling polices. Here, GS: greedy scheduler; QS: queue-length based proportional fair scheduler; RS: random scheduler.

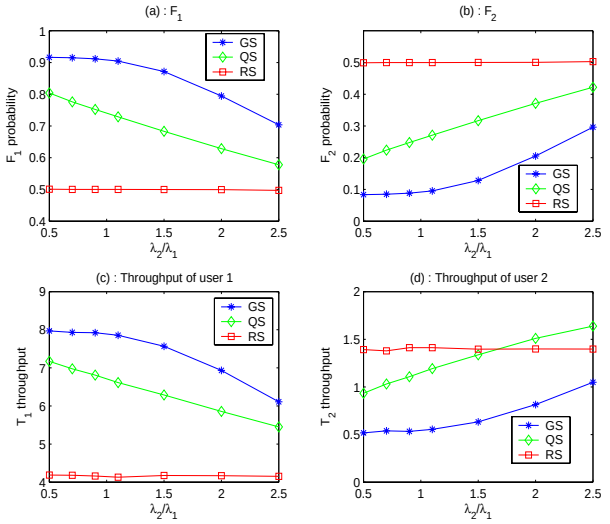

Fig. 8. Effect of user's locations on fairness and capacity of a wireless data network. Here, GS: greedy scheduler; QS: queue-length based proportional fair scheduler; RS: random scheduler.

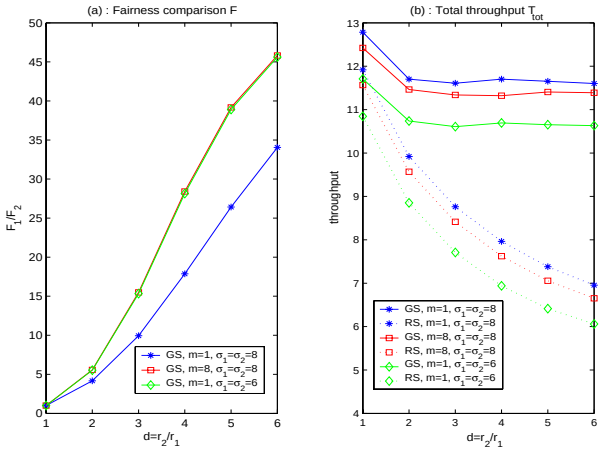

Fig. 9. Effect of log-normal shadowing and Nakagami fading on the fairness and capacity of wireless data networks. Here, GS: greedy scheduler; RS: random scheduler.